

RSC Advances



This is an *Accepted Manuscript*, which has been through the Royal Society of Chemistry peer review process and has been accepted for publication.

Accepted Manuscripts are published online shortly after acceptance, before technical editing, formatting and proof reading. Using this free service, authors can make their results available to the community, in citable form, before we publish the edited article. This *Accepted Manuscript* will be replaced by the edited, formatted and paginated article as soon as this is available.

You can find more information about *Accepted Manuscripts* in the [Information for Authors](#).

Please note that technical editing may introduce minor changes to the text and/or graphics, which may alter content. The journal's standard [Terms & Conditions](#) and the [Ethical guidelines](#) still apply. In no event shall the Royal Society of Chemistry be held responsible for any errors or omissions in this *Accepted Manuscript* or any consequences arising from the use of any information it contains.



ARTICLE

Smart Poly(aniline-formaldehyde) Microcapsules Based Self-healing Anticorrosive Coating

J. Yamuna, T. Siva, S. Sreeja Kumari and S. Sathiyarayanan*

Received 00th January
20xx,

Accepted 00th January
20xx

DOI: 10.1039/x0xx00000x
www.rsc.org/

Abstract: Effectiveness of linseed oil and mercaptobenzothiazole (MBT) encapsulated poly(aniline-formaldehyde) [PAF] microcapsules was investigated for healing of cracks generated in paint/coatings. Microcapsules were prepared by *in situ* polymerization of aniline-formaldehyde resin to form shell over linseed oil and mercaptobenzothiazole. Characterization of these capsules were studied by FTIR, TGA, Scanning Electron Microscope (SEM). EIS studies at the artificial defect area have shown that the coating containing microcapsules is able to protect steel in neutral media since the impedance values remained at $1.287 \times 10^8 \Omega \text{cm}^2$ even after 15 days exposure where as the coatings without microcapsules have lost their protection ability. The self healing ability of the coating containing microcapsules was studied by SVET.

1. Introduction

Corrosion of metals causes substantial financial losses and requires extensive efforts to limit its impact. For pipeline systems for example, uncontrolled corrosion may induce leaks, fire and explosion among others consequences.¹⁻³ Results of a studies showed that the total annual estimated direct cost of corrosion in many nations is approximately between 2 and 5% of the nation's Gross Domestic Product. Hence selecting effective and economical techniques for minimizing the effects of corrosion is a critical design decision. Spending 90% of corrosion protective methods and services costs for protective coatings⁴ emphasized the necessity for attention to this corrosion control method. There is a great variety of corrosion protective coatings which can be broadly divided into metallic, inorganic, and organic coatings. Organic coatings have a wide usage in miscellaneous industry. Paint as an organic coating was developed to protect damages due to corrosive environment.^{5,6} Encapsulation of functionally active materials in hollow microspheres is an attractive way of storing as well as protecting the functionally active materials from environment till required for fulfilling appropriate applications. Microencapsulated substances have been utilized for sustained drug release,⁷ electro rheological

fluids,⁸ intumescent fire retarding powders,⁹ preservation of flavours,¹⁰ electro phoretic display applications,¹¹ textiles,¹² biotechnology¹³ and inorganic metal salt catalyst¹⁴, etc. Recently, there has been growing interest in use of microencapsulated materials for healing of cracks generated during service of a polymer based composite materials.¹⁵

Paints are extensively used for modification of substrates either for aesthetic appearance or for corrosion protection. During its service life, the paint film undergoes changes in mechanical /chemical properties leading to formation of microcracks which subsequently propagates and exposes substrate to atmospheric moisture and oxygen. This action results in accelerated disbonding of the paint and flake formation from the metal coating interface. Paint coatings can be considered as a special class of composite materials, comprising binders and pigments. Hence, the concept of self-healing of cracks, as reported for composites, can be adopted for coatings to provide longer durability. An attempt for healing of scratches on automotive coating using temperature dependant elastic properties of polymer has been reported.¹⁶

The microcapsules are tiny particles with diameters in the range of nanometers to micrometer consisting of core materials and covering shell.¹⁷ Microcapsules can encapsulate various substances including gases, liquids, solids, etc. Encapsulating shell material can also be selected from a wide variety of natural or synthetic polymers depending on the desired characteristics of the

CSIR-Central Electrochemical Research Institute, Karaikudi 630006, India.
*Corresponding author. Tel.: +91 4565 241390.
E-mail addresses: sathya@cecri.res.in

microcapsules. By tuning the composition of core materials, it is possible to endow microcapsules with a variety of functions. Recently the microencapsulation technology exhibited significant promise by providing “smart” functionality for applications such as self healing composites.¹⁸ Aniline formaldehyde (AF), a rigid and slowly degradable polymer which can be prepared by *in situ* polymerization in aqueous solutions is an appropriate shell material.¹⁹ Linseed oil is one of the most widely used drying oils in paints formulation. Drying oils are natural triglycerides containing high percentage of polyunsaturated fatty acids with air-drying property. These polyunsaturated fatty acids readily oxidize to form a three-dimensional network.²⁰

Although tremendous endeavours have been invested in the research of microcapsules based selfhealing anticorrosive coating, active agent loaded PAF type microcapsule has not been reported so far. Here, we have reported the synthesis of PAF microcapsules loaded with linseed oil and MBT(mercaptobenzothiazole) [LO/MBT] and self healing behavior of this microcapsules containing epoxy coating. Our work is devoted for a better understanding of the reaction parameters that influence the microencapsulability of the core material. The PAF shell material was opted as it avoids leakage and diffusion of the encapsulated active agent for a prolonged time. In order to evaluate the relation between the experimental conditions and the encapsulation yield, a set of PAF micro-capsules containing LO/MBT was prepared in which reaction time, temperature and stirring speed were modulated. Scanning Electron Microscopy (SEM) was used to investigate the microcapsule size and surface morphology. Optical microscopic observation and Scanning Vibrating Electrode Technique (SVET) were used to evaluate the self healing properties of microcapsules containing coating.

2. Experiment

2.1. Materials

Linseed oil was purchased from Hindustan Produce Company, Kolkata, and mercaptobenzothiazole (MBT) was purchased from Sigma Aldrich Chemicals, Mumbai. Aniline and formaldehyde aqueous solutions, acting as shell forming monomers, were obtained from TCI Chemical Reagent Co. Ltd., Mumbai. Ammonium chloride (NH₄Cl), and resorcinol used to maintain the pH (base condition) were purchased from Fisher Scientific Chemicals, Mumbai. Dodecylbenzenesulphonic acid (DBSA) purchased from

Sigma Aldrich Chemicals, Mumbai was used as an emulsifier. Hydrochloric acid (HCl) purchased from Merck; Mumbai, was used to control the pH of solution (acid condition). Commercial grade epoxy resin 6071 (CibaGeigy India Ltd.), polyamide hardener (Synpol-125), Methyl isobutyl ketone (MIBK), xylene and acetone were used without further purification. All solutions were prepared using Millipore double distilled water having resistivity 18.2 MΩ cm.

2.2. Synthesis of microcapsules

Microencapsulation is a technique through which liquid materials either aqueous or non-aqueous in nature is encapsulated within solid shell. The nature of shell wall materials is a function of the material to be encapsulated, the coating application process. Microcapsules were prepared by *in situ* polymerization in an oil in water emulsion. At room temperature, 250 mL of water and 10 mL of DBSA were taken in a three neck round bottom flask and agitated for 30 min using a magnetic stirrer (stirring bar 8 mm dia × 25 mm long) at 1200 rpm. 20 mL of aniline, 0.5 g of ammonium chloride and 0.5 g of resorcinol were mixed using magnetic stirrer at room temperature. After the aniline was completely dissolved, the pH of the solution was adjusted to 8-9 with 1.0 M NaOH and the temperature was kept at 50-55°C for 30 min. A slow stream of prepared mixture (5:1) of LO (25 g)/MBT (5 g) was added to form an emulsion and allowed to stabilize for 10 min. After stabilization, the pH of the emulsion was adjusted to 2-3.5 by the slow addition of hydrochloric acid. 12.76 mL aqueous solution of formaldehyde (1.7 M) was then added to the emulsion while heating the solution at a rate of 1 °C min⁻¹ to the target temperature of 50–55 °C. The emulsion was covered and slowly heated and maintained at 55 °C using magnetic stirrer at 200 rpm for 4 h. The reaction was completed after 4 h. Contents were cooled to ambient temperature. Microcapsules from the suspension were recovered by filtration under vacuum. These microcapsules were rinsed with water, washed with xylene to remove suspended excess oil. The capsules were dried under vacuum.

2.3. Determination of core content by using Soxhlet method

The core content within the microcapsules was determined by using soxhlet apparatus. A known weight of microcapsules (W_0) was crushed using pestle and mortar and transferred to a thimble of known weight (W_1), pestle and mortar were rinsed with xylene and added to thimble. Extraction was carried out using xylene as a solvent, extracted for 1 h and finally dried in a vacuum oven at 70 °C. The final weight of the thimble (W_2) was noted. Eventually the

core content (A) of the microcapsules was calculated by the following equation.^{21,22}

$$A (\%) = \frac{(W_0 + W_1) - W_2}{W_0} \times 100$$

2.4. Characterization of inhibitor loaded poly(aniline-formaldehyde) microcapsules

2.4.1. FTIR spectroscopy: The FTIR spectra of LO/MBT loaded PAF microcapsules and PAF microcapsules containing epoxy coating was recorded using Nicolet 380 (Thermo, USA) FTIR instrument having ATR attachment. The self healing process by the release of core materials was confirmed by recording the FTIR at the scratched area using a Nicolet Centaurus FTIR Microscope.

2.4.2. Nuclear Magnetic Resonance Analysis: ¹H Nuclear Magnetic Resonance (¹H-NMR) spectra were recorded on a Bruker Avance spectrometer, corresponding to the resonance frequency of 400 MHz for the ¹H nucleus, equipped with a direct detection four nuclei probe head and field gradients on Z axis.

2.4.3. Thermal analysis of microcapsules: Microcapsules, linseed oil, mercaptobenzothiazole and aniline-formaldehyde resin were analyzed using Thermal Analyzer STA in nitrogen environment with a sample weight of about 3mg. Heating rate was maintained at 20 °C/min in the temperature range of 30–800 °C.

2.4.4. Morphology studies: The microcapsule formation at various reaction time was observed under an optical microscope and morphology of PAF microcapsule was analyzed using Zeiss scanning electron microscope.

2.5. Preparation and application of poly(aniline-formaldehyde) microcapsules containing paint

The epoxy resin (6071; Ciba Geigy) solution was prepared by dissolving solid epoxy having epoxy equivalent weight 450–500 in xylene. PAF microcapsules (3 g) were completely dispersed in the resin using attritor at ambient temperature. The PAF microcapsules containing epoxy resin solution was cured by polyamide (Sympol 115) having amine value 210–230 mg KOH/g (by HClO₄ method). The ratio of resin to hardner is 3:1. The paint was prepared in such a way that it had 30% volume solids and 10% PAF microcapsules volume concentration. The paint was prepared in such a way with different concentration of microcapsules. Clean mild steel panels, size 150 mm × 100 mm × 2 mm after wire brushing were coated by brush to obtain an average dry film thickness. The coatings were evaluated after 10 days of curing at room temperature. The

thickness of the coating was measured using a coating thickness metre (Elcometer 456) and it was found to be 100 ± 5 μm. The stability of the microcapsules in paint will long for more than 30 days but after the curing period, the specimens were subjected to electrochemical impedance spectroscopic (EIS) studies.

2.6. Evaluation of poly(aniline-formaldehyde) microcapsules containing paint

2.6.1. EIS evaluation of dual active agent loaded poly(aniline-formaldehyde) in epoxy coating

EIS measurements were conventionally used to evaluate the performance of organic coatings. Since the purpose of this study is to evaluate the self healing properties of microcapsules, EIS measurements were conducted in the scratched area of both the epoxy alone and LO/MBT loaded AF microcapsules containing paint coated panels, using the three electrode corrosion cell constructed at the scribed spot by adding a platinum foil counter electrode using Electrochemical Impedance Analyzer (PAR, 2273). Impedance measurements were carried out using Power sine software in a frequency range of 100 kHz to 0.1 Hz with an AC signal of rms amplitude of 20 mV for different exposure time duration in 3.5% NaCl. The measurements were carried out with triplicate samples and the measured impedance values are reproducible to ±3 to 5%. From the impedance plots, the coating resistance (R_c) and the coating capacitance (C_c) values were calculated using Zsimpwin 3.21 software where C_c is the coating capacitance and R_c is the coating resistance.

2.6.2. Self healing property evaluation

The scanning vibrating electrode technique (SVET) instrumentation used in these experiments was from Princeton Applied Research (SCV 370 control unit) described in detail elsewhere. Samples prepared for SVET measurement were of 1 cm × 1 cm squares with scan area of 4000 μm × 4000 μm and 6 4 × 48 points X and Y-axes. The coated samples were scribed to introduce an artificial defect of size ranging from 0.1 to 0.3 mm². The sample was mounted in a teflon holder and the 3.5% NaCl solution was added. Scans were initiated within 5 min of immersion and the data were collected for various durations. Each scan consists of 400 data points on a 20 × 20 grid, with an integration time of 1 s per point. A complete scan required 10 min, followed by a 5 min rest period prior to the next scan. The current density maps were plotted in 3D format over the scan area, with positive and negative current densities representing

anodic and cathodic regions, respectively. The measurements were taken at the open circuit potential.

3. Results and discussion

3.1. Mechanism of poly(aniline-formaldehyde) capsules formation

Poly(aniline-formaldehyde) shell is formed by the reaction of two reactants such as aniline and formaldehyde. The condensation of formaldehyde with aniline has been examined by a number of authors, mainly from a synthetic viewpoint. The products of the reaction depend on the pH of the reaction medium.

Initially an *N*-(hydroxymethyl)amine, or carbinolamine, **1** is formed. This then dehydrates to give an unstable imine, **2**, which immediately polymerises to give a cyclic trimer (**3**, path **a**) or reacts with another amine molecule to give a dinuclear species (**4**, path **b**) (see Fig. 1).²³

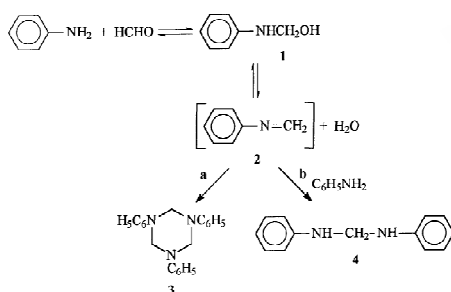


Fig. 1. Mechanism of PAF microcapsule formation.

3.2. FTIR study

Microcapsule prepared from aniline-formaldehyde resin (shell material) and filled with linseed oil and MBT (core material) were characterized using FTIR. The spectrum of aniline-formaldehyde resin recorded is reported in Fig. 2a. The band at 3463 cm^{-1} corresponds to N-H stretching with hydrogen bonded amino groups and free O-H stretching vibration and is attributed to N-H stretching vibration.²⁴ Peak at 3030 cm^{-1} is due to aromatic C-H stretch. The C-H stretch in formaldehyde generally comes at 2850 cm^{-1} . It confirms that the presence of $-\text{CH}_2$ moiety in aniline-formaldehyde unit. Prominent spectral features are observed at 1621 and 1360 cm^{-1} are for N-H bending and C-N aromatic stretching, respectively, confirming the presence of the primary and secondary amine moiety. A strong absorption band at 1601 cm^{-1} is due to aromatic C=C ring stretching which also supports the probable structure of aniline-formaldehyde. Few absorption frequencies are broad due to the presence of by products in the resin, such as water and excess formaldehyde.²⁵

Figure 2b shows the FTIR spectra of the aniline-formaldehyde microcapsules loaded with linseed oil alone. The spectrum is dominated by a series of aliphatic vibrations around 3009 cm^{-1} , due to the presence of large amount of $-\text{CH}_2$ and $-\text{CH}$ group in fatty acid. The main stretching absorption bands were observed for ester C=O (1745 cm^{-1}) and ester C-O (1374 cm^{-1} and 1278 cm^{-1}).²⁶

In the case of PAF loaded with LO/MBT (Fig. 2c), the band at 3450 cm^{-1} is due to NH-stretching mode indicates the presence of thione form of MBT molecules. The peak at 2654 cm^{-1} indicates the S-H stretching vibration of MBT. The strong bands observed in the FTIR spectra at frequencies 1020 and 1090 cm^{-1} are ascribed to N-C-S group vibration in addition to C-H bending vibration of MBT thione form. The absorption band observed at 1567 and 1482 cm^{-1} is assigned to the non-symmetric vibration mode of C=C in quinoid and benzenoid ring system in polyaniline.

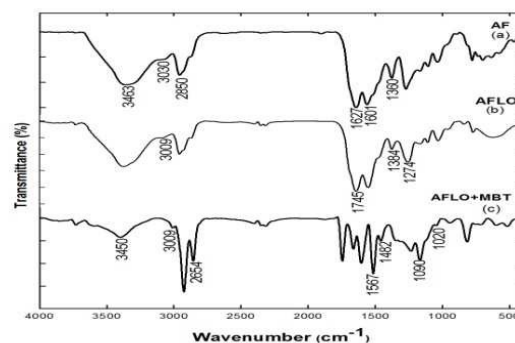


Fig. 2. FTIR spectrum of (a) aniline-formaldehyde resin, (b) aniline-formaldehyde+LO and (c) PAF microcapsule.

3.3. ¹H-NMR Analysis

Microcapsules prepared were characterized using ¹H-NMR. The spectrum of PAF and pure linseed oil is shown in Fig. 3. The peak at 5.3 and 7.2 shows the presence of linseed oil and MBT in the PAF capsules. From the recorded spectral data, the presence of core content inside the capsule was confirmed.

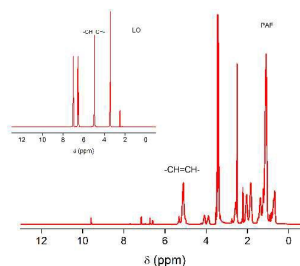


Fig. 3. $^1\text{H-NMR}$ spectrum of PAF microcapsule.

3.4. TG Analysis

TG analysis of active agent loaded PAF microcapsule, aniline-formaldehyde with linseed oil and aniline formaldehyde are shown in Fig. 4a. In all the cases, the thermogram showed three stages of degradation. The first stage of degradation in the temperature region of 80–273, 55–153, and 52–220°C respectively for PAF microcapsule, aniline-formaldehyde with linseed oil and aniline formaldehyde indicates the evaporation of moisture. The second and third stage for AF shell started at 220–430°C and continued up to 600°C. This is attributed to the degradation of cross linked polymer and AF resin. In the case of AFLO, the microcapsules have initial decomposition in the range 220–443°C which continued up to 520°C due to decomposition of linseed oil, shell materials of the microcapsules. The second and third stage degradation of PAF microcapsule occurs in the temperature between 273 and 564°C. This is attributed to the decomposition of shell material, core material and cross linked polymer formed by the rapid exothermic polymerization reaction of core material.

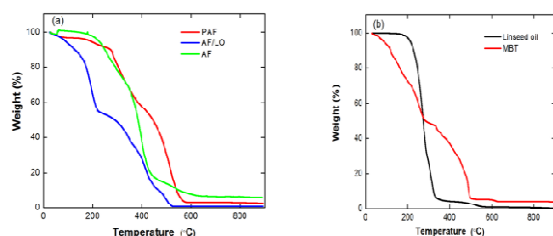


Fig. 4. TG analysis of (a) active agent loaded PAF microcapsule, aniline-formaldehyde with linseed oil and aniline formaldehyde and (b) LO and MBT.

The thermal degradation of linseed oil and mercaptobenzothiazole commences at 200–400°C is also shown in Fig. 4b. In general, from thermogravimetric analysis, it is concluded that the thermal stability is high in the case of AF shell compared with PAF microcapsules. It also indirectly confirms the existence of inhibitor in the microcapsules.

3.5. Optical microscopic studies

The morphology of microcapsules synthesized in different time durations were studied using optical microscope and the results are presented in Fig. 5a-e. As can be seen in Fig. 5a-e the shell thickness

increases with increasing reaction time, thereby leading to an increase in the permeability of the shell wall. One of the possible reasons which can be attributed to increased permeability is a facile polymerization reaction for shell formation at the interface in the direction normal to the surface of the core. This facilitated increase in the shell thickness.²⁷ So as to form a compact-nonporous shell. It is reported that the combination of the reaction time and stirring speed (1200 rpm), allows formation of microcapsules with a maximum core having thin and compact shell wall thickness.²⁸

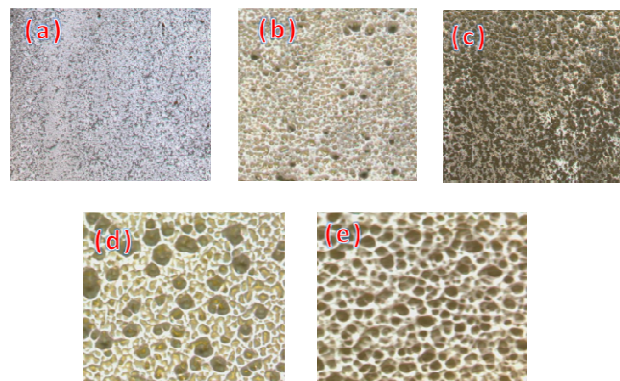


Fig. 5. Optical Microscopic images of active agent loaded PAF microcapsule during various time of synthesis (a) 5 minutes; (b) 15 minutes; (c) 30 minutes; (d) 45 minutes and (e) 60 minutes.

3.6. Analysis of microcapsule using SEM

The surface morphology and shell wall thickness of the capsule were analysed by SEM. Fig. 6a and b shows the surface morphologies of the microcapsules; that had the rough exterior shell wall. Some microcapsules were ruptured to allow for viewing of the inner shell wall morphology and thickness of the microcapsules are investigated. Polymerization between aniline and formaldehyde is initiated and a low molecular weight pre-polymer is formed in the water phase. As the molecular size increases, the polymer deposits in the organic/aqueous interface which is constituted by the formaldehyde monomer. The polymerization continues resulting in a high cross linked aniline formaldehyde capsules wall in the presence of resorcinol and ammonium chloride. The formation of PAF capsules is thus attributed to the precipitation of higher molecular weight pre-polymer in the aqueous solution and their agglomeration and deposition on the active agent droplet surface.

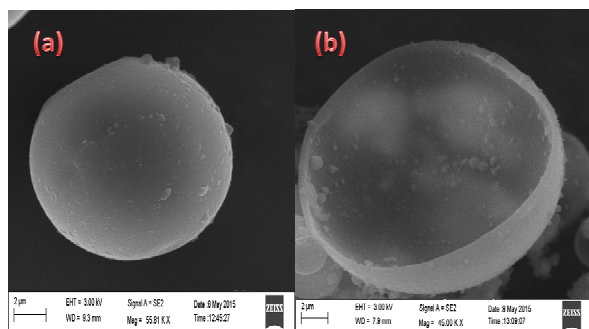


Fig. 6. SEM images of the microcapsules (a), the rough exterior shell wall (b) view of a ruptured microcapsule.

The shell thickness increases with excess amount of ammonium chloride or resorcinol, addition of small core materials, uniform stirring and lower initial pH. The shell wall thickness is 10 nm over the full range of microcapsule diameters investigated.

3.7. Analysis of self healing process

SVET was used to study the self healing property of the microcapsules. After 10 days of curing, an artificial defect was induced by using razor blade. Coated substrate was immediately transferred under the lens of optical microscope to record the healing performance by the release of core materials from the microcapsules with LO/MBT. It is observed that the initial width of the crack is maximum as shown in Fig. 7b. This crack width gets reduced and completely filled after 1 h (Fig. 7c). From the Soxhlet apparatus we have estimated that the core content of PAF microcapsules is 82%. Inhibitor loaded linseed oil has the ability to dry by oxidation with atmospheric oxygen and hence sealed the crack in the coating.²⁹

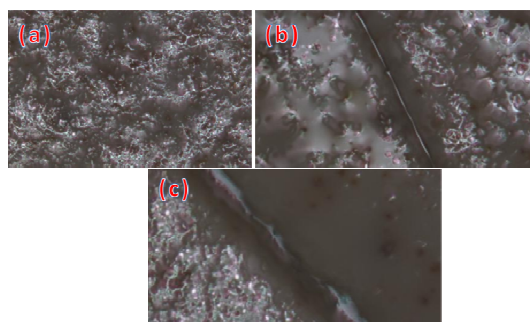


Fig. 7. Optical Microscopic images of healing performance of PAF microcapsules. (a) Before crack; (b) After crack; (c) After 1 h healed by crack blocker

FTIR recorded at the sealing part is shown in Fig. 8a. The peak at 1468 and 1382 cm^{-1} represent the bending vibration of (CH, CH_2) moieties present in linseed oil released from the microcapsules. Presence of thione form of MBT molecules is also confirmed by a peak at 3455 cm^{-1} in the FTIR spectra recorded in the defect area. These evidences aid us to conclude that the self healing of defect is due to the release of LO/MBT from microcapsules.

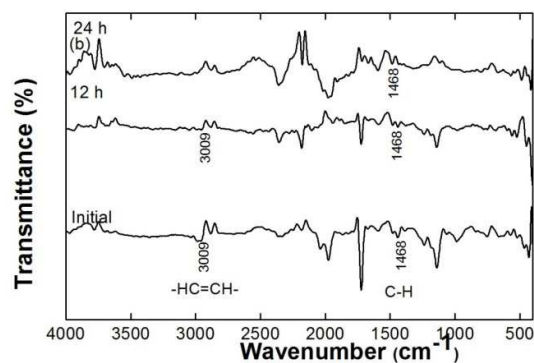
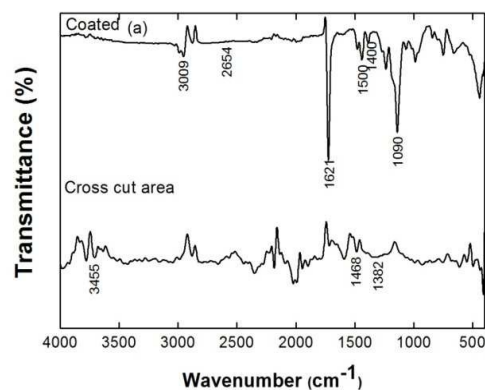


Fig. 8. (a) FTIR Spectrum of (a) PAF microcapsule loaded paint panel, (b) linseed oil curing.

In the case of linseed oil curing by air, the vibrations of the $-\text{C}=\text{C}-$ group of LO have been followed (Fig. 8b). Initially the main characteristic of alkene bands occurs at 3009 cm^{-1} . During this period, it is also observed that there is a decrease in the intensity of the peak of $-\text{C}=\text{C}-$ group at 3009 cm^{-1} indicating the air drying of LO. At the end of measurement, i.e. after 24 h the intensity of this characteristic alkene bands completely disappeared linseed oil by air oxidation.

3.8. Corrosion protection evaluation

3.8.1. EIS study

The performance of the coatings was studied by EIS on the sample immersed in 3.5% NaCl. The EIS result are depicted in Figs. 9 and 10 as Bode plots. The impedance parameters such as coating resistance (R_c) and coating capacitance (C_c) derived from these curve are given in Tables 1 and 2.

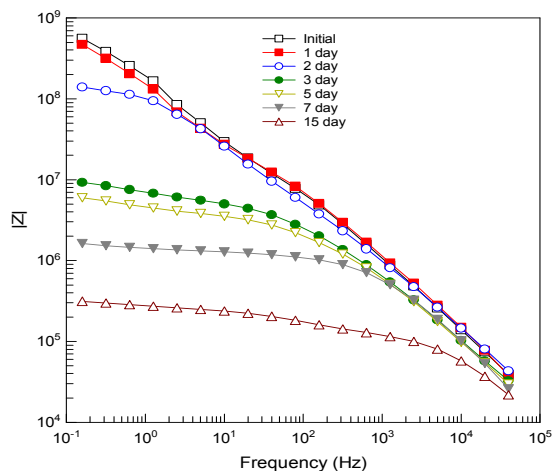


Fig. 9. Impedance behavior (at the scratched area) of epoxy coating on mild steel in 3.5% NaCl.

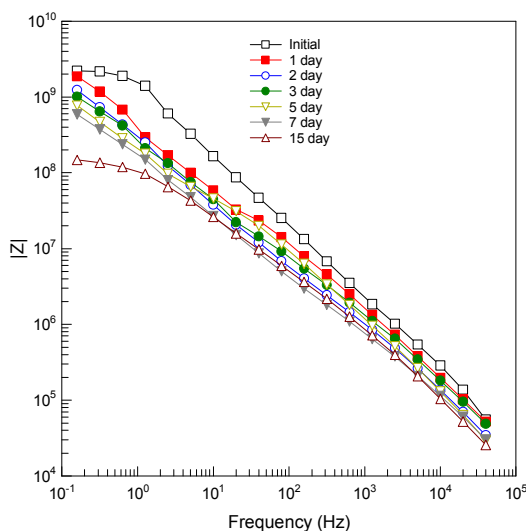


Fig. 10. Impedance behavior (at scratched area) of PAF microcapsule containing epoxy coating on mild steel in 3.5% NaCl.

Period (days)	Coating capacitance, C_c ($F\ cm^{-2}$)	Coating resistance, R_c ($\Omega\ cm^2$)
Initial	5.732×10^{-10}	6.903×10^8
1 Day	7.692×10^{-10}	5.973×10^8
2 Day	4.891×10^{-10}	1.418×10^8
3 Day	1.326×10^{-10}	9.131×10^6
5 Day	1.445×10^{-10}	5.776×10^6
7 Day	5.347×10^{-10}	1.42×10^6
15 Day	1.572×10^{-10}	3.007×10^5

Table 1. EIS parameters at the scratched area in the epoxy coating on mild steel in 3.5% NaCl

Period (days)	Coating capacitance, C_c ($F\ cm^{-2}$)	Coating resistance, R_c ($\Omega\ cm^2$)
Initial	6.972×10^{-10}	2.734×10^9
1 Day	1.183×10^{-10}	2.209×10^9
2 Day	2.005×10^{-10}	1.297×10^9
3 Day	5.543×10^{-10}	1.158×10^9
5 Day	1.474×10^{-10}	1.084×10^9
7 Day	1.505×10^{-10}	8.192×10^8
15 Day	1.847×10^{-10}	1.287×10^8

Table 2. EIS parameters at the scratched area in the PAF microcapsule containing epoxy coating on mild steel in 3.5% NaCl

The impedance performance of epoxy coating without PAF microcapsule on mild steel in 3.5% NaCl solution is shown in Fig. 9. The coating resistance (R_c) and coating capacitance obtained from these curve of the coating with time are given in Table 1. Initially, the R_c is $6.903 \times 10^8\ \Omega\ cm^2$ and with time the R_c value gradually decreases. Finally this value is decreased to $3.007 \times 10^5\ \Omega\ cm^2$ after 15 days of immersion. This decrease in the R_c values over the period of measurement is associated with the degradation of coating.

The impedance spectra of PAF microcapsules containing epoxy coated steel are shown in Fig. 10. In this case it is found that the

ARTICLE

Journal Name

coating has an initial coating resistance of $2.734 \times 10^9 \Omega\text{cm}^2$ which is higher than that of conventional cured epoxy and with time it decreases slowly. Finally at the end of evaluation, i.e. after 15 days the coating resistance value was $1.287 \times 10^8 \Omega\text{cm}^2$ which is two orders above the threshold value of $10^6 \Omega\text{cm}^2$. It is also worth nothing that this final value of coating resistance is higher than that of PAF free epoxy coating indicating the better performance of PAF. These result shows that microcapsules incorporated have improved the protective nature of coating.

3.8.2. SVET studies

The SVET results of conventional PAF cured epoxy coating on steel surface in 3.5% NaCl for various durations of exposure are given in Figs. 11a-d and 12a-d respectively. Fig. 11a depicts the local current maps over the surface of the mild steel coated by conventional PAF cured epoxy recorded immediately after exposure to 3.5% NaCl (i.e. after 5 min). A steep anodic current flow in the flaw area as shown in the Fig.11a indicates the occurrence of accelerated corrosion. With continued exposure, the corrosion activity at the defect areas spreads laterally as evidenced by the increase in width of the current flow pattern in 1 hour and 12 hour exposure (Fig 11b & c). After 24 h (Fig. 11d) of exposure, more corrosion got initiated at various locations over the coating as seen by the occurrence of thin anodic current flow at various spots (Fig 11d).

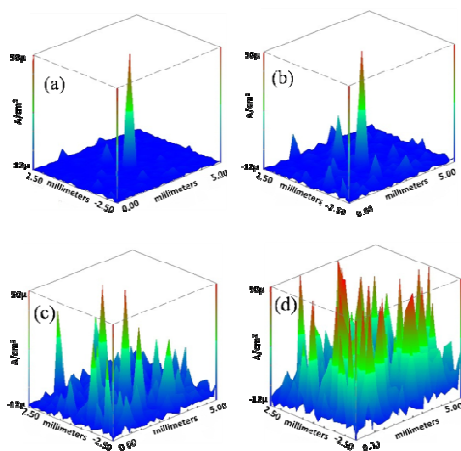


Fig. 11. Current distribution map for pure epoxy coated steel in 3.5% NaCl at various immersion periods (a) initial; (b) 1 h; (c) 12 h; (d) 24 h

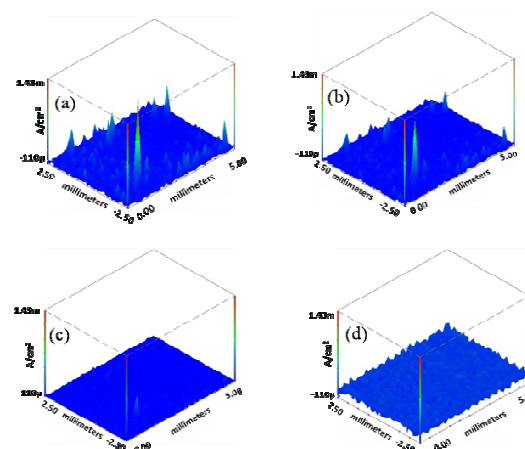


Fig. 12. Current distribution map for PAF microcapsule containing epoxy coating in 3.5% NaCl at various immersion periods (a) initial; (b) 1 h; (c) 12 h; (d) 24 h.

Fig.12a shows the SVET current mapping at the initial instant of measurement in the case of PAF microcapsule cured epoxy coating. As shown, there is an anodic current flow at the defect area. Fig 12b shows the current density map after 1 hour immersion in 3.5% NaCl at which time the anodic current flow area decreases dramatically at the defect area. With continuous monitoring, i.e. up to 24 h, (Fig. 12c–d) it was observed that the anodic current flow at the defect area get suppressed and maintained at very low current flow. Visually it was observed that the defect is covered with a dark passive film. This clearly demonstrates the self healing property of PAF microcapsules over steel surface.

4. Conclusion

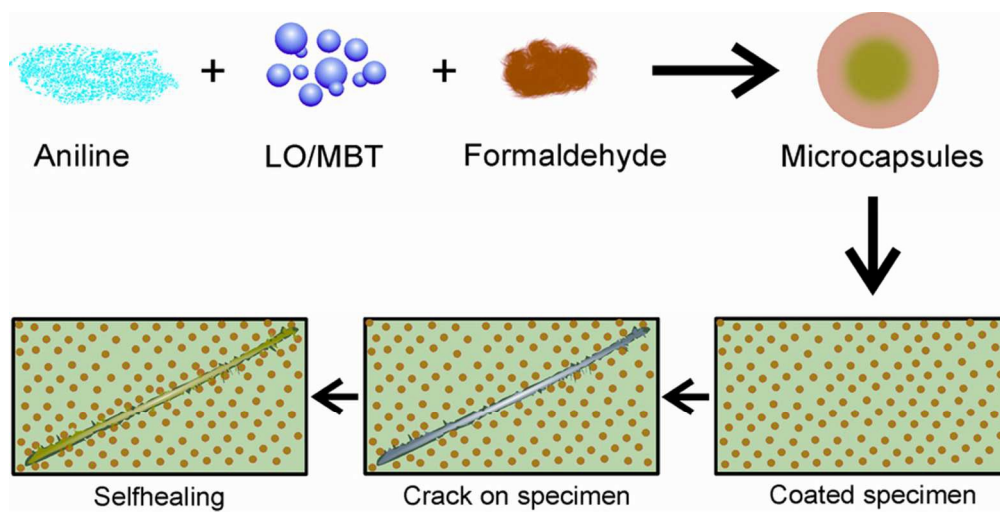
The inhibitor (MBT) mixed linseed oil has been successfully encapsulated into aniline-formaldehyde shell. Core and shell material of the microcapsules were characterized by using FTIR and TG analysis. The observation of microcapsules by optical microscopy confirmed the spherical shape and more importantly, the absence of agglomerates. SEM micrographs confirmed the shell thickness around 10 nm. Soxhlet method estimated 82% of LO and MBT. The PAF microcapsules incorporated epoxy coating was found to offer better corrosion protection than that of microcapsules free epoxy coating. SVET results show the self healing ability of the microcapsules containing coating system as evidenced by the suppression of initial anodic current flow at the defect area.

Acknowledgements

The authors thank the Director, CSIR – CECRI for his permission to carry out this work and also thank CSIR, New Delhi for financial support through 12 FYP Project Intelcoat (CSC0114). I would also like to thank Dr. V. Saranyan for his graphical representation.

References

- 1 E. Bardal, *Corrosion and Protection*, Springer, 2003.
- 2 R. Winston Revie, *Corrosion and Corrosion Control*, 4th ed., John Wiley & Sons, New Jersey, 2008.
- 3 P.R. Roberge, *Corrosion Engineering*, McGraw-Hill, 2008.
- 4 M. Kutz, *Handbook of Environmental Degradation of Materials*, 2nd Ed., William Andrew, 2005.
- 5 W. Zeno and Wicks Jr., *Organic Coatings*, 3rd Ed., John Wiley & Sons, New Jersey, 2007.
- 6 D. Stoye, *Paints, Coatings and Solvents*, 2nd Ed., Wiley-VCH, 1998.
- 7 J. Eukaszczuk and P. Urba, *React. Funct. Polym.*, 1997, **33**, 233–239.
- 8 Y.H. Lee, C.A. Kim, W.H. Jang, H.J. Choi and M.S. Jhon, *Polymer*, 2001, **42**, 8277–8283.
- 9 D. Saihi, I. Vroman, S. Girand and S. Bourbigot, *React. Funct. Polym.* 2005, **64**, 127–138.
- 10 X.D. Liu, T. Ataroshi, T. Furuta, H.F. Yoshii, S. Ashima, M. Okiawara and P. Linko, *Drying Technol.*, 2001, **19**, 1361–1374.
- 11 B.J. Park, J.Y. Lee, J.H. Sung and H.J. Choi, *Curr. Appl. Phys.*, 2006, **6**, 632–635.
- 12 G. Nelson, *Int. J. Pharm.* 2002, **242**, 55–62.
- 13 G. Sukhorukov, A. Fery, and H. Möhwald, *Prog. Polym. Sci.* 2005, **30**, 885–897.
- 14 H.B. Ji, G.J. Kuang and Y. Qian, *Catal. Today* 2005, **105**, 605–611.
- 15 E.N. Brown, M.R. Kessler, N.R. Sottos and S.R. White, *J. Microencapsul.*, 2003, **20**, 719–730.
- 16 C. Challener, *JCT*, January 2005, pp. 50–55.
- 17 S. Benita, *Microencapsulation Methods and Industrial Applications*, 2nd ed., Taylor & Francis, CRC Press, Philadelphia, 2006.
- 18 B.D. Park, S.M. Lee and J.K. Roh, *Eur. J. Wood Prod.*, 2009, **67**, 121–123.
- 19 K.S. Ho, T.H. Hsieh, C.W. Kuo, S.W. Lee, J.J. Lin and Y.J. Huang, *J. Poly. Sci. Part A: Poly. Chem.*, 2005, **43**, 3116–3125.
- 20 P.D. Tatiya, R.K. Hedao, P.P. Mahulikar and V.V. Gite, *Ind. Eng. Chem. Res.*, 2013, **52**, 1562–1570.
- 21 R.S. Jadhav, D.G. Hundiware and P.P. Mahulikar, *J. Appl. Polym. Sci.*, 2010, **119**, 2911–2916.
- 22 R. Wang, H. Li, H. Hu, X. He and W. Liu, *J. Appl. Polym. Sci.*, 2009, **113**, 1501–1506.
- 23 B. Kathryn Helen, *Kinetic studies on the reaction of formaldehyde with amines in the presence of sulfite*, Durham theses, Durham University, 1999.
- 24 R. Khan, P. Khare, B. Prasad Baruah, A.K. Hazarika and N. Chandra Dey, *Adv. Chem. Eng. Sci.*, 2011, **1**, 37–44.
- 25 T. Maity, B.C. Samanta and S. Dalai, *Pig. Res. Technol.*, 2006, **35**, 12–21.
- 26 R.S. Jadhav, V. Mane, A.V. Bagle, D.G. Hundiware, P.P. Mahulikar and, G. Waghoo, *Int. J. Ind. Chem.*, 2013, **31**.
- 27 Y. Song, P. Sun, L.L. Henry and B. Sun, *J. Membr. Sci.*, 2005, **251**, 67–79.
- 28 R. Finken and U. Seifert, *J. Phys.: Condens. Matter*, 2006, **18**, L185–L191.
- 29 J. Mallegol, J. Lemaire and J.L. Gardette, *J. prog. Org. Coat.*, 2000, **39**, 107–113.



40x19mm (600 x 600 DPI)